Solid Freeform Fabrication 2023: Proceedings of the 34th Annual International Solid Freeform Fabrication Symposium – An Additive Manufacturing Conference
Reviewed Paper

DETERMINATION OF INPUT LASER ENERGY FOR MELTING POWDER LAYERS OF VARIOUS THICKNESSES IN HIGH-SPEED PBF-LB/P USING NEAR-INFRARED LASER AND ABSORBENT

Yuki Yamauchi*, Takashi Kigure*†, and Toshiki Niino†

*Tokyo Metropolitan Industrial Technology Research Institute, Aomi, Koto-ku, Tokyo, 135-0064
†Institute of Industrial Science, the University of Tokyo, Komaba, Meguro-ku, Tokyo, 153-8505

Abstract

The rate of production of PBF-LB/P can be increased by increasing the layer thickness. However, this reduces the part resolution in the stacking direction. To obtain both a high rate of production and high part resolution, layer thickness adjustment in accordance with part geometry can be effective. Optimizing the input laser energy with respect to the layer thickness ensures sufficient melting and part strength. According to previous studies, the use of a near-infrared laser and absorbent can increase penetration depth or depth of fusion. However, the optical properties of the powder bed can vary significantly depending on the layer thickness, and, therefore, the input energy that actually contributes to melting also changes with layer thickness. This study proposes a method for determining the input laser energy for various layer thickness without trial and error by estimating the amount of energy required to melt the powder layer while accounting for the optical properties of the bed.

Introduction

Powder bed fusion with laser beam and polymeric material (PBF-LB/P), an additive manufacturing technology using polymeric materials with relatively high productivity and high part reliability, is increasingly being adopted as a production method for end-use parts; it reduces the number of assembly processes and reproduces complex shapes [1]. However, the productivity of PBF-LB/P is significantly lower than that of injection molding, the process which is currently used. This results in high component costs, hindering its widespread use. To improve the productivity of PBF-LB/P, it is necessary to increase the build process speed. This can be achieved by shortening the time required to create each layer[2] or by reducing the number of layers per part. The number of layers required to build each part can be reduced by increasing the layer pitch (nominal layer thickness) [3][4][5][6], although the layer pitch is closely related to the part resolution in the stacking direction. As proposed here (see Figure 1), by adjusting the stacking pitch according to the part shape, the number of layers can be reduced while maintaining the resolution of the part. As the layer pitch changes, the amount of powder used in each layer and the thickness of the powder layer change. As the powder layer thickness increases, more energy is required to melt it and it becomes more difficult to connect it with the layer underneath [7][8]. Since the melting condition of the powder and the adhesion between the layers directly affect the mechanical properties of the built part[9], an appropriate amount of laser energy should be supplied to sufficiently melt the powder layers of various thicknesses. Also, high energy input to melt thick (deep) powder layers may cause thermal degradation of the polymer near the surface of the powder layer[10][11][12][13]. This is especially important for light that is highly absorbed, such as a CO_2 laser, which has low penetration through the powder layer[14][15]. Previous research by the authors has shown that increasing the laser transmittance increases the melting depth while minimizing thermal degradation[16]. Therefore,

for processes employing variable powder layer thickness, an increase in the transmittance of the laser is an effective solution. However, the method employed by the authors to adjust the transmittance of a near-infrared laser – the use of an absorber – results in a large loss of energy due to diffuse reflection, which varies depending on the powder layer thickness. Therefore, the layer thickness and optical properties must be considered to systematically and efficiently determine the appropriate input laser energy. The authors have modified EMR (Energy Melt Ratio which is the ratio of the amount of energy required to melt the powder material and the amount of input laser energy, proposed by Starr et al. [9]) taking into account the loss of energy due to the reflection and transmission of laser light in the powder bed, and have attempted to quantitatively determine the amount of input laser energy [17]. In addition, the relationship between the modified EMR and the part density, which is strongly correlated with its mechanical properties, was investigated and was found to be good and stable regardless of the various conditions, such as the optical properties of the powder bed. In other words, it is possible to determine the input laser energy for various layer pitches by maintaining the modified EMR value proposed by the authors. In this study, we determined the amount of input laser energy for a given and fixed modified EMR value for various layer pitches without trial and error, and investigated the relationship between the layer pitch and the mechanical properties of the built part.

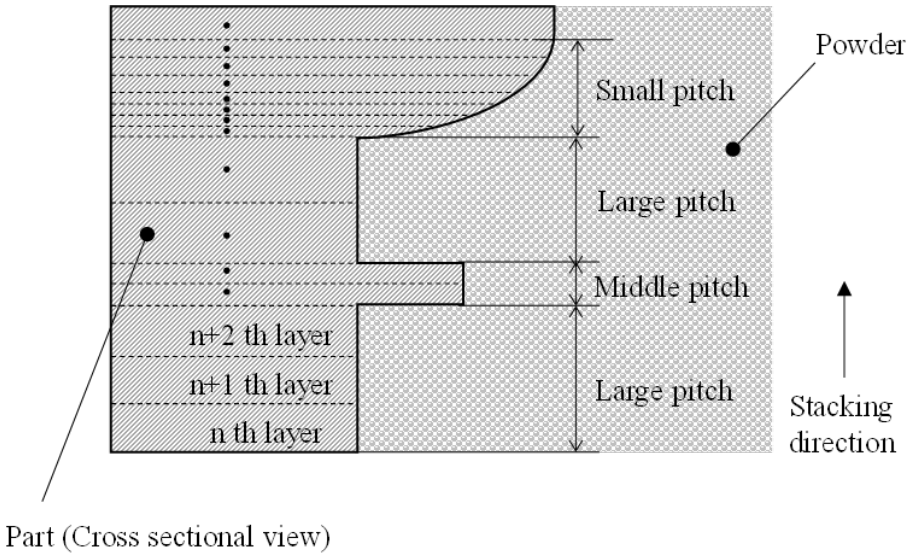

Figure 1 Schematic of layer pitch adjustment in a part

Methods and Materials

Methodology

For melting thick powder layers without thermal decomposition near the surface, the depth up to which the incident laser beam reaches, i.e., the penetration depth, should be larger than that of a CO_2 laser. In this study, to increase the penetration depth, we used a near-infrared laser, which permeates most polymeric materials and added an absorber to the powder material for absorbing near-infrared light, as mentioned earlier. For highly transmissive and reflective powder beds, we introduce the modified EMR proposed by the authors (see Equation 1) as a modified index of the EMR used by Starr et al.[9] to quantify the amount of input laser energy per layer, considering the optical properties.

$$EMR_m = \frac{E_{vm}}{E_{pm}} = \frac{(1 - R_0 - R_z) \times \frac{P}{y \times v} \times \left(1 - e^{-\frac{z}{D_p}}\right)}{\left[C_p(T_m - T_b) + h_f\right] \times \rho_p \times z}, \quad (1)$$

where, R_0,R_z, P, y, v, D_p, C_p, T_m, T_b, h_f, ρ_p, and z are the specular reflectance at the powder bed surface, diffuse reflectance at the powder layer thickness z, laser power, scan spacing, scan speed, penetration depth, specific heat capacity, melting point, powder bed temperature, melting heat capacity, density of the powder material, and thickness of the powder layer, respectively. By keeping the modified EMR value for each layer pitch constant as a reference, the quantitative input laser energy can be matched even if the layer pitch changes. The modified EMR values used in this study were determined based on the relationship between various modified EMR values and the part density which is closely related to melting. Tensile tests were conducted on the built specimens to check whether the part strength could be maintained constant while changing the layer pitch and unifying the modified EMR values. In this study, specifically, the tensile strength in the stacking direction, which is strongly affected by an increase in layer pitch, was evaluated.

Materials

PA11 (ASPEX-FPA, Aspect Inc.) was used as the powder material, and 0.4 wt% of a coloring agent (Nubian Black PC-0870, Orient Chemical Industry Co., Ltd.) was added in powder form to the PA11 powder to assist laser light absorption in the near-infrared region. C_p, T_m, T_b, ρ_p, and h_f for this material, were referenced from the specifications of a similar material [18] and were set to 2.09 J/g K, 200°C, 0.45 g/cm^3, and 83.7 J/g, respectively.

Optical properties measurement

The optical properties of the powder material used in this study, including R_0,R_z, and D_p, were measured for the modified EMR calculation in same manner as proposed in the authors' previous report [8] [17]. The thickness of the powder layer was calculated from the weight of the powder filled in the container and the bulk density of the powder. The container consisted of quartz glass and a stainless steel plate with a 50 mm diameter hole. The volume of the container and the amount of powder filled were adjusted by changing the thickness of the stainless steel plate. The powder layer formed on the container was irradiated by a laser beam with a diameter of 1.5 mm and a wavelength of 1.06 μm. The light passed through the powder layer and the bottom of the container (quartz glass), and the transmitted light was measured with a power meter. Transmittance is the ratio of the energy transmitted through the powder layer and the incident energy. Diffuse reflectance was measured simultaneously with transmittance measurements using a barium sulfate-coated integrating sphere and the same light source, container, and powder material as for transmittance measurements. To

compensate for the loss of energy caused by the integrating sphere, the diffuse reflectance of the powder layer was determined from the ratio to a reference specimen of known reflectance (99.6%).

Powder layer thickness

In this study, we make a clear distinction between layer pitch and powder layer thickness. Because the low bulk density of the powder results in the formation of a powder layer thicker than the layer pitch in the next layer due to consolidation by melting and flow [19][20]. Consolidation is considered in the powder layer thickness z as shown in the equation below:

$$z \cong z_i \frac{\rho_m}{\rho_p} \tag{2}$$

where, z_i and ρ_m are layer pitch and density of the melting region, respectively. Note that the layer thickness can be greater than this equation for the first few layers, as shown below. In the melting process of the first layer, the laser beam is irradiated into a very thick powder layer, since there is no previously processed layer. Therefore, the melting depth and consolidation depth can be greater, leading to recoating of the thicker powder in the next layer. Therefore, this equation is valid when the recoating process has been done with several layers.

Specimen preparation

A laser sintering machine (RaFaEl300F, Aspect Inc.) equipped with a near-infrared laser (wavelength = 1.06 μm) was used to build the specimens. Specimens for the density measurements were 10 × 10 × 5 mm in size, with a layer pitch of 100 μm and a modified EMR ranging from 1.2 to 3.2. The process parameters are shown in Table 1. The powder bed temperature was set at 140°C, which is lower than the process window. According to the authors' previous study, when the powder bed temperature is low, especially below the process window, bonding between the processing layer and the previously processed layer becomes difficult. This means that we can easily observe the effect of changes in layer pitch on the bonding process under the bed temperature below the process window. Therefore, the powder bed temperature was set below the process window in this study.

For a high-speed processing, the laser beam is scanned as fast as possible, and then the high laser power is required to fill the input energy for appropriate melting. However, the maximum laser power of the machine used in this study is not sufficient, so a slow scanning speed was used.

Contour scanning was not performed for the following reasons: it does not have a large effect on the part density of the fabricated part, and for the tensile test specimen, the surface was removed by milling or polishing before the tensile test.

Table 1 Process parameters

Parameter	Set point
Bed temperature (°C)	140
Layer pitch (μm)	100
Laser power (W)	15~45
Scan speed (m/s)	2
Scan interval (mm)	0.07

Based on the results of the density evaluation described below, specimens for tensile testing were fabricated for a layer pitch range of 100-300 μm with a modified EMR of approximately 1.7, the minimum value at which the part density saturates.

Part density

A relative density of the built part was obtained to know the melt state. The relative density is the ratio of the density of the part to the true density of the material used; the absorbent is not included in the calculation because its concentration is negligibly small. The density of the built part was measured based on the Archimedes method.

Tensile test

Tensile tests were performed using a universal testing machine (INSTRON 3366, 10 kN load cell). Tensile specimens were of standardized geometry and 1/2 scale, that is 75 × 10 × 2 mm. The longitudinal side of the specimen was oriented in the stacking direction (z axis). The crosshead travel speed was set at 2 mm/min according to the specimen size. To suppress the influence of surface roughness on the tensile test result, the specimen surface was removed by milling or polishing before the test as mentioned above.

Results and Discussion

Optical properties

Figure 2 shows the relationship between the powder layer thickness and transmittance. Assuming that the attenuation of the laser light incident on the powder layer is based on the Beer-Lambert law [21], the measured values were approximated by an exponential curve. The penetration depth obtained from the approximate curve was 225 μm. According to previous reports, the penetration depth of CO_2 lasers is 80 to 100 μm [14][15], which is less than half as deep as that in this study.

Figure 3 shows the relationship between the powder layer thickness and diffuse reflectance. The reflectance increases with the powder layer thickness and tends to saturate above 300μm. Assuming that the diffuse reflection in this study follows the Kubelka-Munk theory [22], an approximate curve can be obtained as shown in the figure from which the diffuse reflectance at a given thickness can be obtained. For all thicknesses, it can be seen that the diffuse reflectance is very high for the method used in this study compared to that of the CO_2 laser, which has been reported to be less than 5% [14][23], indicating that the energy loss due to reflection must be considered. Additionally, specular reflection was also obtained by the previously reported method [17] and was approximately 8%.

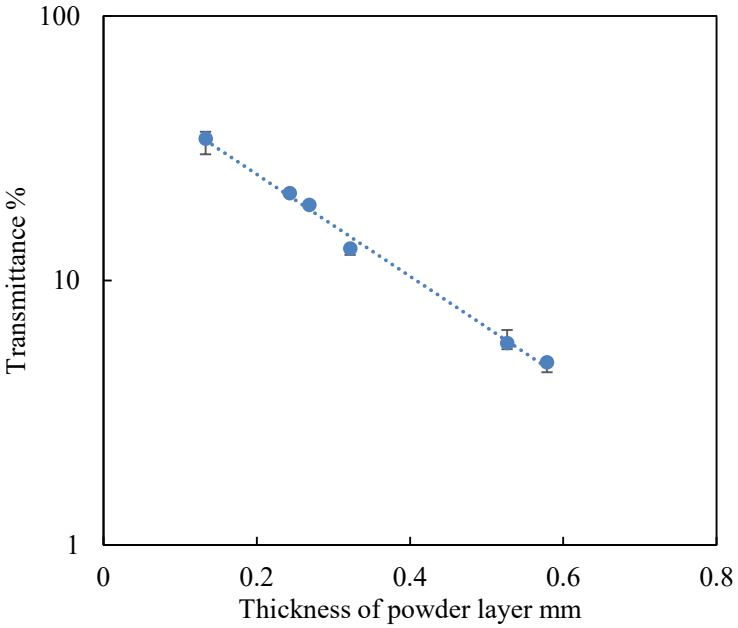

Figure 2 Relationship between powder layer thickness and transmittance. Error bars were obtained from the maximum and minimum values of the experiment for n = 5.

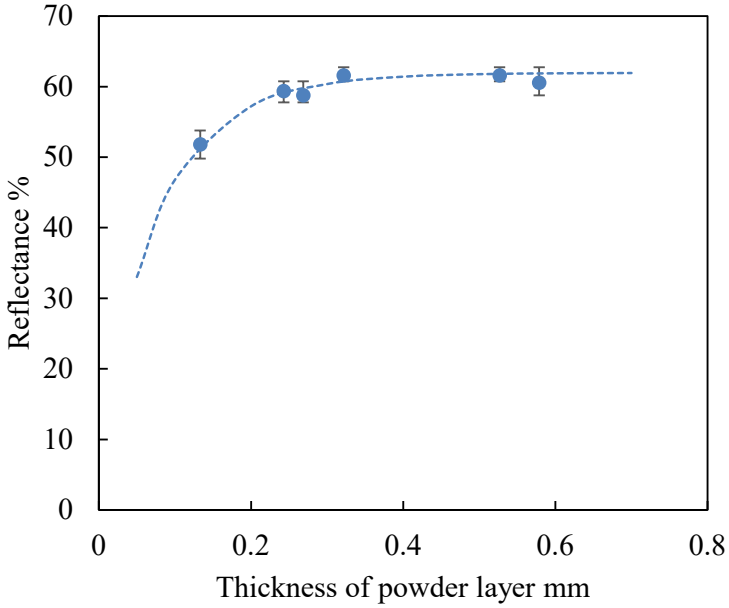

Figure 3 Relationship between powder layer thickness and diffuse reflectance. Error bars were obtained from the maximum and minimum values of the experiment for n = 5.

Part density

Figure 4 shows the relationship between the modified EMR and the relative density of the built specimens. The results show that the relative density of the parts saturates when the modified EMR is greater than 1.5. Theoretically, the powder should melt at a modified EMR of 1, but because of the energy required for coalescence and flow, a modified EMR greater than 1 is required to increase the density.

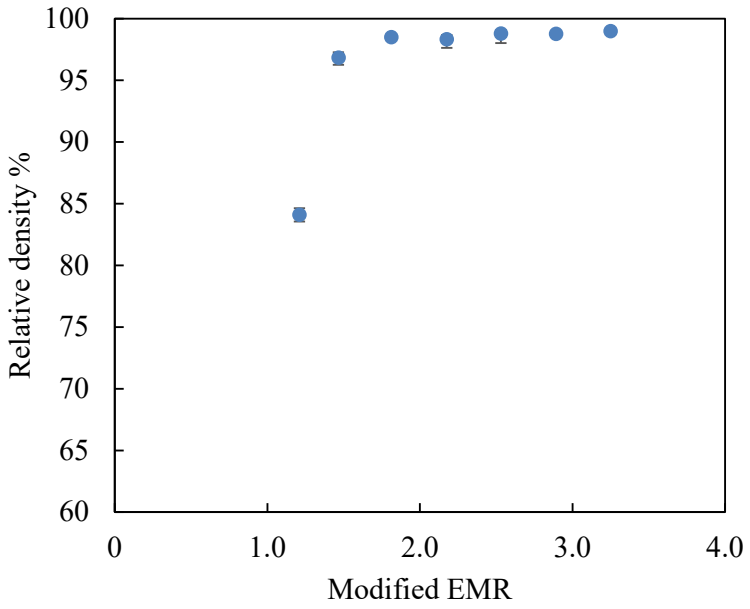

Figure 4 Relationship between modified EMR and relative density of built specimens. Error bars were obtained from the maximum and minimum values of the experiment at n = 5.

Tensile test

Figure 5 shows the relationship between the layer pitch and ultimate tensile strength (UTS). For layer pitch values from 100 to 250 µm, the UTS remains almost flat at about 35 MPa, showing that the same modified EMR value can be used to build parts with similar strengths. When the layer pitch is 300 µm, the UTS is about 30 MPa, which is 15% lower compared to the other values. With respect to the Young's modulus result, as shown in Figure 6, it appears to be generally close to the UTS result. The decrease in Young's modulus begins above 250 µm pitch, which is slightly different from the UTS result. There is also almost the same trend in elongation at break as the UTS result, except for the 150 µm pitch (see Figure 7).

Figure 8 shows the cross sections of the samples with different layer pitches. Voids can be seen for all pitches. However, the 300 µm pitch specimen has more regularly positioned voids which might have reduced its strength in the stacking direction.

The result of the tensile test and void formation are discussed below. As stated earlier, the laser penetration depth of the powder bed in this study was 225 µm. But, for each layer, the powder layer thickness in the processed area is approximately 2.3 times the layer pitch, based on the relationship between the layer pitch and the density of the specimen as given by equation (2). Therefore, when the layer pitch is 100 µm or greater, the powder layer thickness is greater than the laser penetration depth. Powder in the regions deeper than the penetration depth is heated and melted mainly by heat transfer from the regions where the laser beam penetrates and heats directly. As the layer pitch is increased, the powder in the deeper, impenetrable regions is not sufficiently melted because not enough energy is transferred. This leads to a lack of bonding between the layers. On the other hand, if the input laser energy is increased to melt the deep-seated regions sufficiently, the surface of the powder bed could exceed the thermal decomposition temperature. Therefore, depending on the depth of the powder layer and light penetration, it can be assumed that thermal decomposition at the surface of the powder bed and insufficient melting at the bottom of the powder layer, both, will occur in the same layer as shown in Figure 9. This means that even though it may be necessary to increase the input energy to eliminate insufficient melting, it will not be possible because it would lead to excessive thermal decomposition on the surface. Voids of different shapes are present in the 300 µm pitch

in Figure 8, implying that they were generated by different phenomena. If the previous assumption is correct, some voids are caused by insufficient melting and the others by thermal decomposition.

As can be understood from the previous discussion, it is necessary to make the temperature difference between the surface and bottom of the powder layer as small as possible in order to further increase the layer pitch. To achieve this, it should either be possible to use a low energy input laser or to increase the penetration depth of the powder bed. The first option can be realized by increasing the powder bed temperature, but there is an upper limit to this, and the degradation of the material due to temperature must be fully considered. The second option can be implemented by using a small amount of absorbent to increase the penetration depth. Previous studies by the authors show that the penetration depth of the powder bed can be controlled by a calibration curve, which is a relationship between optical properties (absorbance) and absorbent content (concentration) based on the Beer-Lambert law. For example, in this study, when the absorbent content is reduced to 1/2, the penetration depth is expected to increase to 300 μm. But this also means lower absorption, and so the actual input energy required for processing will be greater.

In addition, the UTS result in this study appears to be slightly lower than other commercially available parts using the same material. To obtain higher UTS, higher interlayer adhesion is required, which might be obtained under higher M-EMR. Therefore, optimizing the M-EMR in this way is important and should be carried out in future studies.

Finally, we tested only one type of material, absorbent and absorbent content in this study. We also need to validate in future study whether the method proposed in this study can be applied to other material.

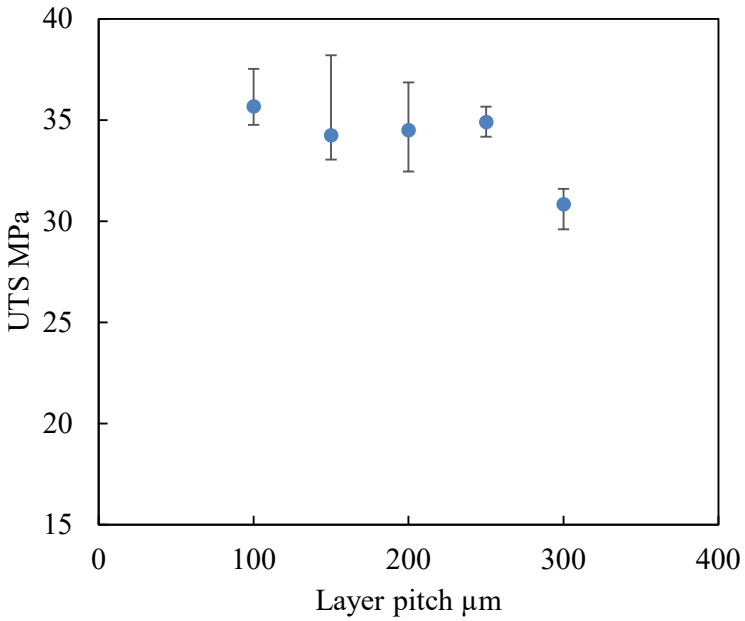

Figure 5 Relationship between layer pitch and UTS under modified EMR of approximately 1.7. Error bars were obtained from the maximum and minimum values of the experiment for n = 5.

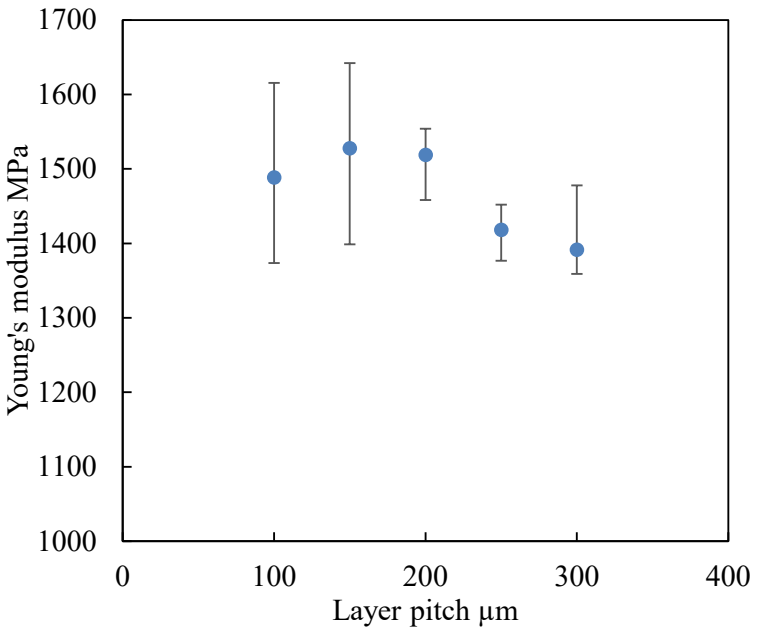

Figure 6 Relationship between layer pitch and Young's modulus under modified EMR of approximately 1.7. Error bars were obtained from the maximum and minimum values of the experiment for n = 5.

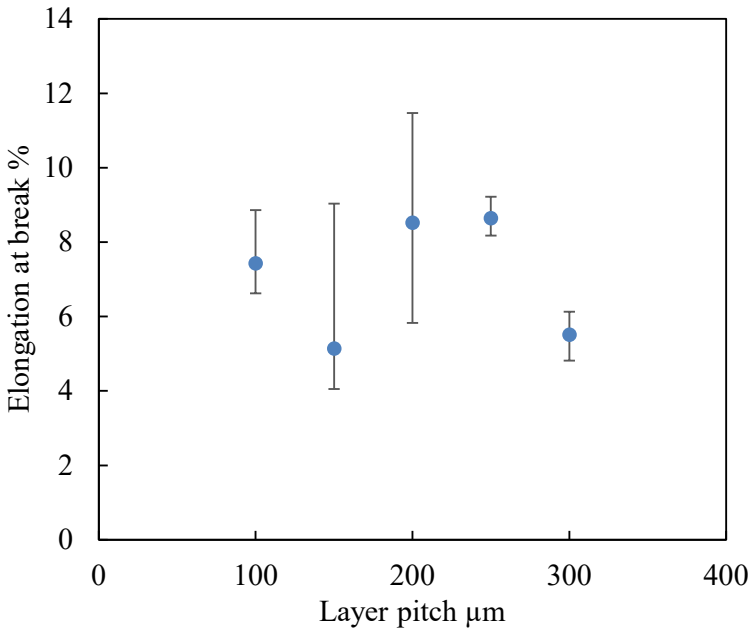

Figure 7 Relationship between layer pitch and Elongation at break under modified EMR of approximately 1.7. Error bars were obtained from the maximum and minimum values of the experiment for n = 5.

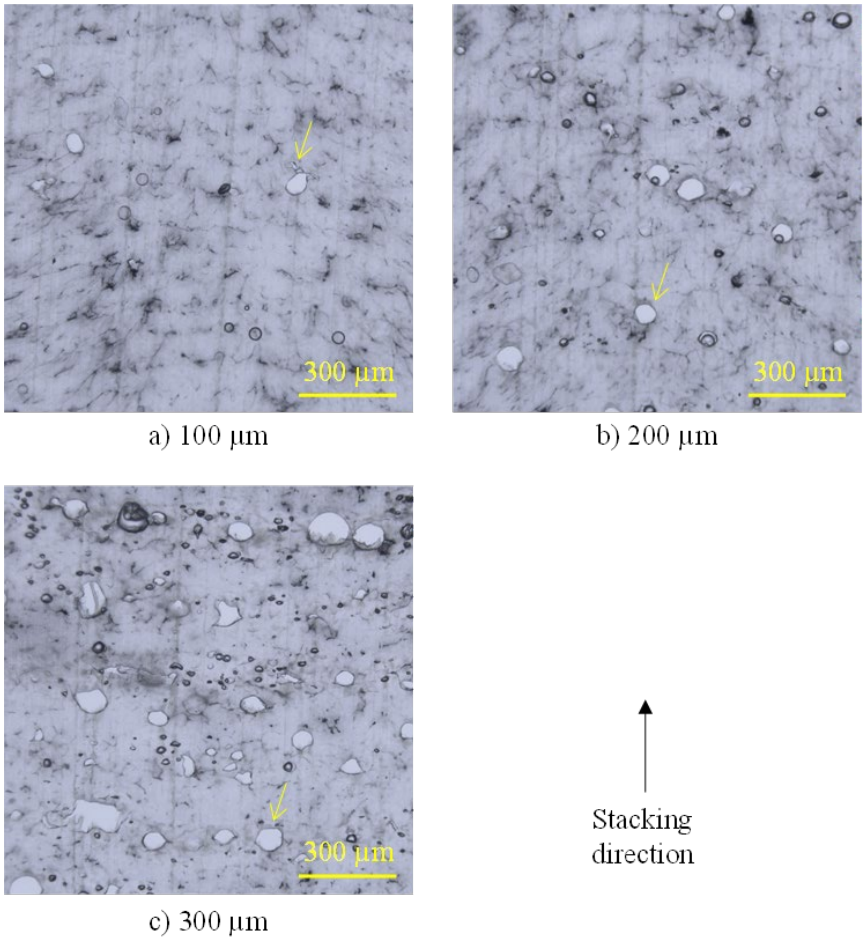

a) 100 µm b) 200 µm

c) 300 µm

Figure 8 Cross sections of build specimens observed under a microscope with transmitted light. One of the voids in each image is indicated by an arrow. 20 µm thick specimens were cut for observation from cross sections of tensile specimens using a microtome.

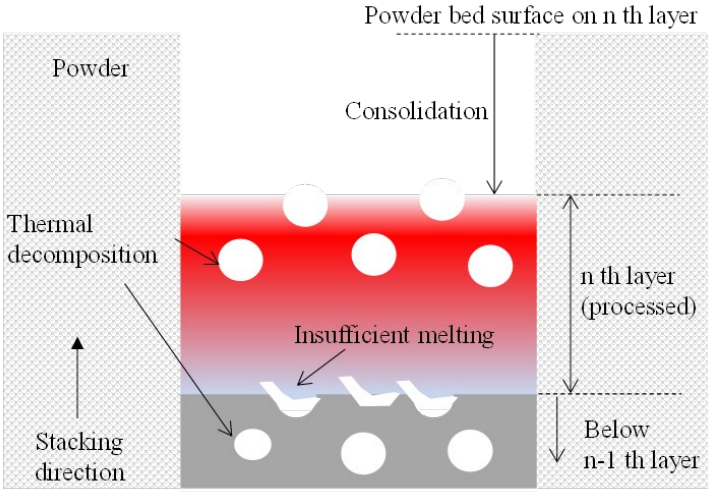

Figure 9 Insufficient melting and thermal decomposition in the same layer. Voiding generated by thermal decomposition results in a spherical shape, while those caused by insufficient melting are distorted and sharply pointed.

Conclusion

In this study, in order to efficiently and systematically determine the input energy of the laser for various layer pitches, the energy absorbed by the powder was quantitatively determined from its optical properties, and the relationship between the modified EMR, which is the ratio of the amount of energy required to melt the powder material and the amount of input laser energy, and the part density was obtained. For the material used in this study, it was found that high-density parts could be built with a modified EMR of 1.5 or higher. Furthermore, the mechanical properties of specimens built with a fixed modified EMR and different layer pitches were evaluated. The results indicate that similar mechanical properties can be obtained when the stacking pitch is 250 μm or less. The results of this study suggest that if the input laser energy is controlled so that the modified EMR becomes a set value for a certain layer pitch or less, it is possible to set the desired layer pitch while retaining the mechanical properties, thereby enabling efficient fabrication and maintaining part resolution.

Acknowledgement

This research was supported by METI R&D Support Program for Growth-oriented Technology SMEs Grant, Number JPJ005698.

Reference

[1] T.D. Ngo, A. Kashani, G. Imbalzano, K.T.Q. Nguyen, D. Hui, Additive manufacturing (3D printing): A review of materials, methods, applications and challenges, Compos. Part B Eng. 143 (2018) 172–196. https://doi.org/10.1016/j.compositesb.2018.02.012.

[2] S. Chowdhury, N. Yadaiah, C. Prakash, S. Ramakrishna, S. Dixit, L.R. Gupta, D. Buddhi, Laser powder bed fusion: a state-of-the-art review of the technology, materials, properties & defects, and numerical modelling, J. Mater. Res. Technol. 20 (2022) 2109–2172. https://doi.org/10.1016/j.jmrt.2022.07.121.

[3] J. Li, S. Yuan, J. Zhu, W. Zhang, S. Li, C. Wang, Numerical investigation of novel process planning in the polymeric powder bed fusion, J. Manuf. Process. 67 (2021) 195–211. https://doi.org/10.1016/j.jmapro.2021.04.060.

[4] C. Schwerz, F. Schulz, E. Natesan, L. Nyborg, Increasing productivity of laser powder bed fusion manufactured Hastelloy X through modification of process parameters, J. Manuf. Process. 78 (2022) 231–241. https://doi.org/10.1016/j.jmapro.2022.04.013.

[5] A. Leicht, M. Fischer, U. Klement, L. Nyborg, E. Hryha, Increasing the Productivity of Laser Powder Bed Fusion for Stainless Steel 316L through Increased Layer Thickness, J. Mater. Eng. Perform. 30 (2021) 575–584. https://doi.org/10.1007/s11665-020-05334-3.

[6] S. Wang, Y. Liu, W. Shi, B. Qi, J. Yang, F. Zhang, D. Han, Y. Ma, Research on high layer thickness fabricated of 316L by selective laser melting, Materials (Basel). 10 (2017). https://doi.org/10.3390/ma10091055.

[7] A. Gullane, J.W. Murray, C.J. Hyde, S. Sankare, A. Evirgen, A.T. Clare, On the use of multiple layer thicknesses within laser powder bed fusion and the effect on mechanical properties, Mater. Des. 212 (2021) 110256. https://doi.org/10.1016/j.matdes.2021.110256.

[8] Y. Yamauchi, T. Kigure, T. Niino, Penetration depth optimization for proper interlayer adhesion using near-infrared laser in a low-temperature process of PBF-LB/P, J. Manuf. Process. 98 (2023) 126–137. https://doi.org/10.1016/j.jmapro.2023.05.006.

[9] T.L. Starr, T.J. Gornet, J.S. Usher, The effect of process conditions on mechanical properties of laser-sintered nylon, Rapid Prototyp. J. 17 (2011) 418–423. https://doi.org/10.1108/13552541111184143.
[10] S. Yuan, J. Li, X. Yao, J. Zhu, X. Gu, T. Gao, Y. Xu, W. Zhang, Intelligent optimization system for powder bed fusion of processable thermoplastics, Addit. Manuf. 34 (2020) 101182. https://doi.org/10.1016/j.addma.2020.101182.
[11] D. Drummer, M. Drexler, K. Wudy, Impact of heating rate during exposure of laser molten parts on the processing window of PA12 powder, Phys. Procedia. 56 (2014) 184–192. https://doi.org/10.1016/j.phpro.2014.08.162.
[12] M. Vasquez, B. Haworth, N. Hopkinson, Optimum sintering region for laser sintered Nylon-12, Proc. Inst. Mech. Eng. Part B J. Eng. Manuf. 225 (2011) 2240–2248. https://doi.org/10.1177/0954405411414994.
[13] M. Vasquez, B. Haworth, N. Hopkinson, Methods for Quantifying the Stable Sintering Region in Laser Sintered Polyamide-12, Polym. Eng. Sci. 53 (2012) 1230–1240. https://doi.org/10.1002/pen.
[14] T. Laumer, T. Stichel, K. Nagulin, M. Schmidt, Optical analysis of polymer powder materials for Selective Laser Sintering, Polym. Test. 56 (2016) 207–213. https://doi.org/10.1016/j.polymertesting.2016.10.010.
[15] F. Osmanlic, K. Wudy, T. Laumer, M. Schmidt, D. Drummer, C. Körner, Modeling of laser beam absorption in a polymer powder bed, Polymers (Basel). 10 (2018) 1–11. https://doi.org/10.3390/polym10070784.
[16] Y. Yamauchi, T. Kigure, K. Isoda, T. Niino, Powder bed penetration depth control in laser sintering and effect on depth of fusion, Addit. Manuf. 46 (2021) 102219. https://doi.org/10.1016/j.addma.2021.102219.
[17] Y. Yamauchi, T. Kigure, T. Niino, Quantification of supplied laser energy and its relationship with powder melting process in PBF-LB/P using near-infrared laser, J. Manuf. Process. 99 (2023) 272–282. https://doi.org/10.1016/j.jmapro.2023.05.002.
[18] Rilsan® Fine Powders and coatings main properties Physical Properties, (n.d.). https://hpp.arkema.com/files/live/sites/hpp_extrememateriales/files/downloads/brochures/rilsan-fine-powders-brochures/rfp-br-physical-properties-rilsan-fine-powders-and-coatings-main.
[19] B. Zhang, J. Ziegert, F. Farahi, A. Davies, In situ surface topography of laser powder bed fusion using fringe projection, Addit. Manuf. 12 (2016) 100–107. https://doi.org/10.1016/j.addma.2016.08.001.
[20] N. Southon, P. Stavroulakis, R. Goodridge, R. Leach, In-process measurement and monitoring of a polymer laser sintering powder bed with fringe projection, Mater. Des. 157 (2018) 227–234. https://doi.org/10.1016/j.matdes.2018.07.053.
[21] L. Xin, M. Boutaous, S. Xin, D.A. Siginer, Numerical modeling of the heating phase of the selective laser sintering process, Int. J. Therm. Sci. 120 (2017) 50–62. https://doi.org/10.1016/j.ijthermalsci.2017.05.017.
[22] V. Džimbeg-Malčić, Ž. Barbarić-Mikočević, K. Itrić, kubelka-munk theory in describing optical properties of paper (I), Tech. Gaz. 18 (2011) 117–124.
[23] M.M. Sun, J.J. Beaman, A Three Dimensional Model for Selective Laser Sintering, 1991 Int. Solid Free. Fabr. Symp. (1991) 102–109.